

ROBUST SPECIFICATION INFLUENCE ON FEEDBACK CONTROL STRATEGIES

Gil-Martínez, M.¹ and García-Sanz, M.²

¹*System Engineering and Automation Group, Electrical Engineering Department,
University of La Rioja. Luis de Ulloa, 20, 26004 Logroño, SPAIN.*

²*Automatic Control and Computer Science Department, Public University of Navarra,
Campus Arrosadía, 31006 Pamplona, SPAIN*

Abstract: The feedback control structures are required in the presence of any kind of uncertainty. The benefits of the feedback are mainly paid with an excessive bandwidth that amplifies the sensor noise, saturating the actuators. This implies the necessity of design trade-offs highly transparent from the Quantitative Feedback Theory. Supposing a given uncertainty for a plant, the set of performance and stability requirements will condition the problem solution. Taking advantage of the QFT bound typology and formulation, the contribution of the robust specification values to their simultaneous achievement will be analysed and particularly as regards the challenging task of the controller design. *Copyright © 2002 IFAC*

Keywords: Robust control, Uncertain dynamical systems, Quantitative Feedback Theory.

1. INTRODUCTION

The feedback control is justified just in the presence of model and/or disturbance uncertainties (Horowitz, 1963). In this case, the benefits of the feedback inevitably have a price. The design trade-offs in a minimum phase SISO feedback control system requires, in terms of the open loop transmission $L=GP$: (a) a low-medium frequency gain $|L|$ high enough for an appropriate robust performance in the reference signal tracking and the disturbance rejection tasks; (b) a $|L|$ decrement as fast as possible with frequency that avoids a large noise amplification mainly at the actuator inputs (Horowitz, 1973); (c) a constraint of the $|L|$ decrement rate by the robust stability requirements.

The feedback control trade-offs are expected to become tougher with an increasing uncertainty size and more ambitious specifications. Supposing a fixed uncertainty, this work is aimed at analyzing the contribution of the specification values to the feedback trade-offs. A quantitative formulation of the problem, such as the Quantitative Feedback Theory (QFT) (Horowitz, 1963) is very helpful in this sense. To be precise, the QFT bounds contain all the information. They stand for the set of control specifications and the plant uncertainty in the Nichols Chart (NC). Therefore, a thorough study of them answers two crucial questions in terms of control theory: the compatibility amongst different robust specifications and the existence of a controller capable of meeting simultaneously all of them.

Several dissertations on the previous questions can be found in: Åstrom (2000a,b), Skogestad and Postlethwaite (1996). The QFT has already offered some answers. Horowitz (1979, App.1) proved the existence of a unique optimum L that satisfies a number of robust specifications, under certain constraints on the plant and on the specifications. Gil-Martínez and García-Sanz (2001) dealt with the simultaneous meeting of the control specifications without those restrictions. Three bound typologies were identified for general feedback purposes and their compatibility was discussed. On the basis of this previous work, the present paper studies more in detail the tolerance contribution to the bound compatibility and, mainly, to the difficulties in the loop shaping step (controller design). Chait and Yaniv (1993) developed bound quadratic inequalities as an aid in the automatic bound computation and the controller design. This bound formulation is used in the present work.

Section 2 covers the general feedback control requirements and includes a quick overview of previous contributions to the bound formulation and classification. Section 3 reviews the bound formulas to identify the influence of each robust specification model on its representative bound. Section 4 is devoted to the difficulties related to the bound compatibility and, mainly, to the feedback controller design as a consequence of the more ambitious specifications.

2. FEEDBACK CONTROL FROM QFT

2.1 Multiple robust control specifications

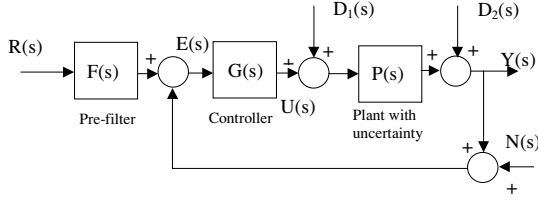


Figure 1: Control structure.

Supposing an uncertain plant, $\{P\}$, and unmeasurable disturbances, $\{D_1, D_2\}$, Figure 1 shows a general two-degrees-of-freedom (Horowitz, 1963) feedback control structure. The controller $G(s)$ must guarantee a robust stability, reduce the closed loop uncertainty and attenuate the input and output disturbances. $G(s)$ also ensures a high frequency gain low enough to minimize the ‘cost of the feedback’ (excessive bandwidth) (Bode, 1945; Horowitz, 1973). Afterwards, the prefilter $F(s)$ shapes the output performance in the reference tracking. Unity feedback is assumed for simplicity.

The QFT outlines the control objectives in the frequency domain and in terms of inequalities (Houpis and Rasmussen, 1999; Yaniv, 1999). Closed loop specification tolerances γ_k are imposed on the system’s transfer functions $|T_k|$ from some inputs to some outputs (see $|T_k|$, $k=1, \dots, 5$ in Table 1). $k=1$ restricts the complementary sensitivity function $|T|=|L/(1+L)$, $L=GP$, implying conditions on the robust stability, the robust control effort in the input disturbance rejection ($|U/D_1|$) and the robust sensor noise attenuation ($|Y/N|$). $k=2$ and $k=3$ constrain the sensitivity functions $|S|=|1/(1+L)$ and $|S|=|P/(1+L)$, respectively, for a robust rejection of the system output ($|Y/D_2|$) and input ($|Y/D_1|$) disturbances. $k=4$ restricts the robust control effort $|G/(1+L)$ for the system output disturbance rejection ($|U/D_2|$), the noise attenuation ($|U/N|$) and the tracking of the reference signals ($|U/R|$). The upper γ_{sup} and lower γ_{inf} models constrain the signal tracking.

Table 1: Feedback control specifications

Transfer functions and specification models	Eq.
$ T_1(j\omega) = \left \frac{L(j\omega)}{1+L(j\omega)} \right = \left \frac{U(j\omega)}{D_1(j\omega)} \right = \left \frac{Y(j\omega)}{N(j\omega)} \right $ $\gamma_1(\omega)$, γ_1	(1)
$ T_2(j\omega) = \left \frac{1}{1+L(j\omega)} \right = \left \frac{Y(j\omega)}{D_2(j\omega)} \right $ $\gamma_2(\omega)$, γ_2	(2)
$ T_3(j\omega) = \left \frac{P(j\omega)}{1+L(j\omega)} \right = \left \frac{Y(j\omega)}{D_1(j\omega)} \right $ $\gamma_3(\omega)$, γ_3	(3)
$ T_4(j\omega) = \left \frac{G(j\omega)}{1+L(j\omega)} \right = \left \frac{U(j\omega)}{D_2(j\omega)} \right = \left \frac{U(j\omega)}{N(j\omega)} \right = \left \frac{U(j\omega)}{R(j\omega)F(j\omega)} \right $ $\gamma_4(\omega)$, γ_4	(4)
$\gamma_{inf}(\omega) \leq T_5(j\omega) = \left F(j\omega) \frac{L(j\omega)}{1+L(j\omega)} \right = \left \frac{Y(j\omega)}{R(j\omega)} \right \leq \gamma_{sup}(\omega)$, γ_5	(5)

2.2 QFT bound formulation and typologies

Considering a particular frequency vector $\{ \omega_i \}$, the QFT translates the closed-loop specifications $\{ \gamma_k(\omega_i) \}$ and the plant templates (boundaries of the uncertain LTI plant at each frequency in $\{ \omega_i \}$, on the NC; Chen and Ballance, 1999) into bounds on the controller

$G(j\omega_i)$ or on the nominal loop transmission $L_0=P_0G$ (Houpis and Rasmussen, 1999; Yaniv, 1999). Chait and Yaniv (1993) developed an iterative algorithm to compute the bounds as follows. Borghesani *et al.*, 1994 implemented it in their software package. Each plant in the i -template can be expressed in its polar form as $P(j\omega_i)=p e^{j\phi} = p \angle \phi$ and, likewise, the controller polar form is $G(j\omega_i)=g e^{j\theta} = g \angle \theta$. Then, substituting and rearranging the inequalities (1) to (5) in Table 1, they are reduced to the quadratic inequalities (6) to (10) in Table 2. For a particular frequency ω_i , there is a constant $k = k(\omega_i)$, and for a fixed plant p in the i -template and a fixed controller phase θ in $[-360^\circ, 0^\circ]$, the unknown parameter of the inequalities in Table 2 is the controller magnitude g . Then, solving equalities such as $ag^2+bg+c=0$ the set of ω_i -bounds for $\{ k=1, \dots, 5 \}$ is computed, leaving apart transitory the uncertainty $\{P\}$.

Table 2: Bound quadratic inequalities

k	Bound Quadratic Inequality	Eq.
1	$p^2 - 1 - \frac{1}{\gamma^2} g^2 + 2 p \cos(\theta + \phi) g + 1 = 0$	(6)
2	$p^2 g^2 + 2 p \cos(\theta + \phi) g + 1 - \frac{1}{\gamma^2} = 0$	(7)
3	$p^2 g^2 + 2 p \cos(\theta + \phi) g + 1 - \frac{p^2}{\gamma^2} = 0$	(8)
4	$p^2 - \frac{1}{\gamma^2} g^2 + 2 p \cos(\theta + \phi) g + 1 = 0$	(9)
5	$p_e^2 p_d^2 - 1 - \frac{1}{\gamma^2} g^2 + 2 p_e p_d p_e \cos(\theta + \phi) - \frac{p_d}{\gamma^2} \cos(\theta + \phi) g + p_e^2 - \frac{p_d^2}{\gamma^2} = 0$	(10)

Gil-Martínez and García-Sanz (2001) introduced the two possible solutions (G -bound formulation) to the quadratic inequalities in Table 2 for each feedback problem in Table 1. See Table 3. Choosing real and positive solutions $g_{1,2}$ in Table 3 as effective controller restrictions, the same authors mentioned four ways to meet the bounds (i.e. the region on the NC to locate g), called typologies (see Figure 2). A bound plotted with a *solid line* implies that $G(j\omega_i)$ (or $L_0(j\omega_i)$) must lie above or on it to meet the particular specification, while a bound plotted with a *dashed line* means that $G(j\omega_i)$ (or $L_0(j\omega_i)$) must lie below or on it.

Table 3: G -bound formulation

k	$g_{1,2}$ bound formulas	Eq.
1	$g_{1,2} = \frac{1}{p} \left[1 - \frac{1}{\gamma^2} \cos(\theta + \phi) \mp \sqrt{\cos^2(\theta + \phi) - 1 + \frac{1}{\gamma^2}} \right]$	(11)
2	$g_{1,2} = \frac{1}{p} \left[\cos(\theta + \phi) \mp \sqrt{\cos^2(\theta + \phi) - 1 + \frac{1}{\gamma^2}} \right]$	(12)
3	$g_{1,2} = \frac{1}{p} \left[\cos(\theta + \phi) \mp \sqrt{\cos^2(\theta + \phi) - 1 + \frac{p^2}{\gamma^2}} \right]$	(13)
4	$g_{1,2} = \frac{1}{p} \left[1 - \frac{1}{p^2 \frac{\gamma^2}{4}} \cos(\theta + \phi) \mp \sqrt{\cos^2(\theta + \phi) - 1 + \frac{1}{p^2 \frac{\gamma^2}{4}}} \right]$	(14)
5	$g_{1,2} = \frac{1}{p_e p_d} \left[1 - \frac{1}{\gamma^2} p_e \cos(\theta + \phi) - \frac{p_d}{\gamma^2} \cos(\theta + \phi) \mp \sqrt{p_e \cos(\theta + \phi) - \frac{p_d}{\gamma^2} \cos(\theta + \phi) - 1 + \frac{1}{\gamma^2} p_e^2 - \frac{p_d^2}{\gamma^2}} \right]$	(15)

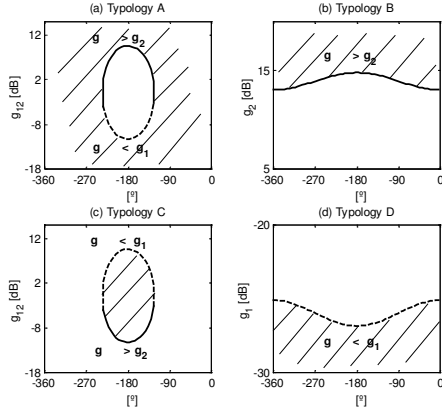


Figure 2: Bound typologies.

Computing the set of $\{g_{12}\}$ for all the i -template $\{p\}$, the less favourable (agreeing the typology), real and positive g_1 and/or g_2 can be calculated. Finally, Table 4 summarises the G -bound formulation and typology for the robust specifications in Table 1; (Gil-Martínez and García-Sanz, 2001). The setting of the bounds on $L_0=P_0 G$ for a nominal plant $P_0 \in P$, rather than on G , is more natural for the loop shaping in QFT. Then, being $L_0(j_i)=l_{0i}$, the L_0 -bounds are simply computed by translating the G -bounds vertically as $|P_0(j_i)|=p_0$ and horizontally as $\angle P_0(j_i)=\theta_i$. The results given for the G -bounds throughout the paper can also be applied to the L_0 -bounds.

Table 4: Bound meeting for general feedback problems

k	$\lambda_i(\omega_i)$	Typ	G -bound meeting; g_1 and g_2 in (11) to (15)
1	$0 < \lambda_1 < 1$	D	$g = \min\{g_1\}$, $g_2 = [-360^\circ, 0^\circ]$
	$\lambda_1 > 1$	A	$g = \max\{g_2\}$, $g_1 = \min\{g_1\}$, $\omega_i \in [180^\circ, 0^\circ]$
2	$0 < \lambda_2 < 1$	B	$g = \max\{g_2\}$, $g_1 = [-360^\circ, 0^\circ]$
	$\lambda_2 > 1$	A	$g = \max\{g_2\}$, $g_1 = \min\{g_1\}$, $\omega_i \in [180^\circ, 0^\circ]$
3	$p > \lambda_3$	B	$g = \max\{g_2\}$, $g_1 = [-360^\circ, 0^\circ]$
	$\{p\} < \lambda_3$	A	$g = \max\{g_2\}$, $g_1 = \min\{g_1\}$, $\omega_i \in [180^\circ, 0^\circ]$
4	$p < 1/\lambda_4$	D	$g = \min\{g_1\}$, $g_2 = [-360^\circ, 0^\circ]$
	$\{p\} > 1/\lambda_4$	A	$g = \max\{g_2\}$, $g_1 = \min\{g_1\}$, $\omega_i \in [180^\circ, 0^\circ]$
5	$\frac{p_{\max}}{p_{\min}} > \lambda_5$	B	$g = \max\{g_2\}$, $g_1 = [-360^\circ, 0^\circ]$
	$\frac{p_{\max}}{p_{\min}} < \lambda_5$	A	$g = \max\{g_2\}$, $g_1 = \min\{g_1\}$, $\omega_i \in [180^\circ, 0^\circ]$

On the basis of this background, the following sections include a wide insight in role of k in the bound compatibility at each frequency and in the skills necessary to loopshape G along the frequency bounds.

3. SPECIFICATION VALUES AND BOUNDS

Checking the G -bound formulas in (11) to (15), note that for a specific compensator phase θ_i , the magnitudes g_1, g_2 are conditioned by the specification value λ_k , and the plant uncertainty: in magnitude $\{p\}$ and phase $\{\theta\}$. The uncertainty is inherent to the nature of the process, and then, it should be considered as it is. On the other hand, the specifications $\lambda_{k=1,\dots,5}$ are design parameters to obtain the best robust performance simultaneously achievable. The contribution of the k -value to the G -bounds is two-folded.

First, λ_k conditions the bound typology (see Table 4). Obviously, the bound type determines the compatibility of the set of ω_i -bounds ($k=1,\dots,5$ bounds).

The other λ_k contribution focuses on the bound aggressiveness in terms of height (g_{12} magnitudes) and width (ω_{12} phase range). In the typology A (Figure 2a), $g = \min\{g_1\}$ and $g = \max\{g_2\}$, $\omega_{12} \in [180^\circ, 0^\circ]$, the bound severity increases when: (a) its existing phase range ω_{12} (ω_i or θ_i) increases, (b) the magnitudes g_1 decrease and the magnitudes g_2 increase at each ω_{12} for $\{p\}$. In the typology B (Figure 2b), $g = \max\{g_2\}$, $\omega_{12} \in [-360^\circ, 0^\circ]$, the bound is more severe when the magnitudes g_2 increase at each ω_{12} for $\{p\}$. In the typology D (Figure 2d), $g = \min\{g_1\}$, $\omega_{12} \in [-360^\circ, 0^\circ]$, the bound hardens when the values g_1 decrease at each ω_{12} for $\{p\}$.

The figures $k=1,\dots,5$ are following analyzed, proving their role on the typology of the bound (bound shape) and on its aggressiveness (bound height and width).

3.1 Specification values on the complementary sensitivity function, $|L/(1+L)|$

As shown in Table 4, depending on the specification value, constant at ω_i as $\lambda_1 = \lambda_1(\omega_i)$, there are two different bound typologies in (11): D for $0 < \lambda_1 < 1$ (Case I), and A for $\lambda_1 > 1$ (Case II). To ensure reasonable phase and gain margins (PM, GM) in terms of robust stability ($|L/(1+L)| < \lambda_1$), a minimum value of $\lambda_1 > 1.3$ is advisable. It ensures $PM \geq 45^\circ$ and $GM \geq 5\text{dB}$ (Chait and Yaniv, 1993). Therefore, a $\lambda_1 = \lambda_1(\omega_i) > 1.3$ at the set $\{\omega_i\}$ ensures that the stability bounds are always of type A (Case II). In general, the specifications for robust sensor noise attenuation ($|Y/N| < \lambda_1$) are watched at high frequencies and usually satisfy $0 < \lambda_1 < 1$, since the noise effect must be attenuated at the output. Then, they provide type D bounds. As regards the control effort allowed for the input disturbance rejection ($|U/D_1| < \lambda_1$), λ_1 can take any value higher than 0, and therefore produce bounds of type B or A.

Case I: $0 < \lambda_1 < 1$, G -Bounds of type D. When the specification value $\lambda_1 = \lambda_1(\omega_i)$ decreases in (11), the magnitude g_1 drops in $[-360^\circ, 0^\circ]$, and then, the bound condition is more severe. See Figure 3a.

Case II: $\lambda_1 > 1$, G -Bounds of type A. Checking (11), a decrease in λ_1 implies, an increase in ω_{12} (bounds at a wider phase band), g_2 rises and g_1 is reduced. Then, the bounds are more severe when the specification figures of merit decrease, as shown in Figure 3b.

In summary, the smaller the specification value is, the more aggressive the corresponding bound in both cases is, namely bounds of type A or D. A decrease in λ_1 also implies a transition to a harder typology (A to D) at $\lambda_1 = 1$. A smaller λ_1 tolerance involves harder restrictions on the stability and the performance: larger phase and gain margins, a smaller control effort for the

disturbance rejection or a higher noise attenuation level required in the output. Its QFT representation through the bounds in Figure 3 shows it.

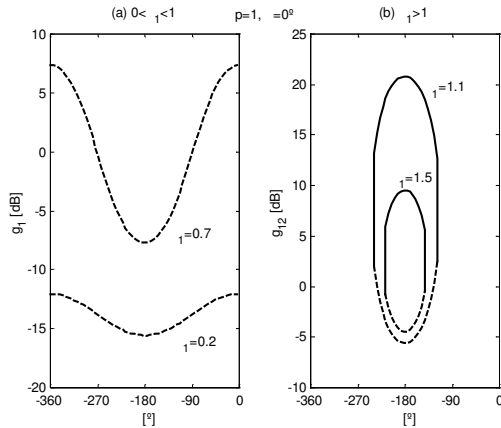


Figure 3: σ_1 influence on its representative bound.

3.2 Specification on the sensitivity function, $|1/D_1| < \sigma_2$

Depending on the specification value at ω_i , $\sigma_2 = \sigma_2(\omega_i)$, two different bound typologies in (12) will appear: B for $0 < \sigma_2 < 1$ (Case I), and A for $\sigma_2 > 1$ (Case II); see Table 4. In line with (2), $|Y/D_1| < \sigma_2$ expresses the robust performance in the rejection of output disturbances. Then, σ_2 usually takes attenuation values $0 < \sigma_2 < 1$, giving type B bounds. The sensitivity values $|S| \ll 1$ at some low frequencies need, at least in practice, that $|S| > 1$ at some moderate high frequencies (Skogestad and Postlethwaite, 1996). This S peak must be constrained by $\sigma_2 > 1$ but close to 1 to ensure minimum gain and phase margins.

Case I: $0 < \sigma_2 < 1$, *G-Bounds of type B.* When the specification σ_2 decreases, the magnitude g_2 increases in $[-360^\circ, 0^\circ]$, and thus the bound condition is more severe. Figure 4a shows these results. Smaller figures of merit σ_2 imply a more aggressive specification in order to obtain a larger D_2 attenuation level at Y .

Case II: $\sigma_2 > 1$, *G-Bounds of type A.* The role of $\sigma_2 > 1$ is the same than the one described in Section 3.1 for the Case I, $\sigma_1 > 1$. Larger stability margins (σ_2 decrement) imply stronger type A bounds. See Figure 4b.

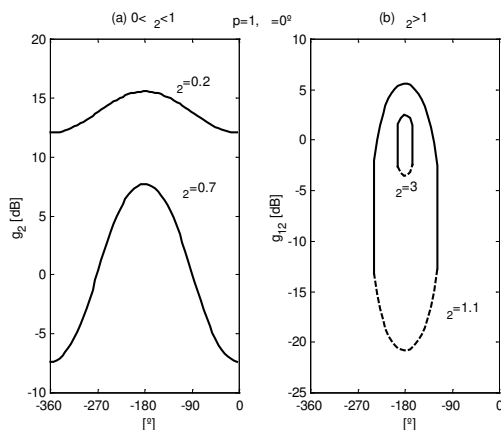


Figure 4: σ_2 influence on its representative bound.

3.3 Specification values on the sensitivity plus the plant function, $|P/1+L| < \sigma_3$

The equation (13) in Table 3 provides two different bound typologies which depend on the relation between the constant specification $\sigma_3 = \sigma_3(\omega_i)$, and the plant magnitude $\{p(\omega_i)\}$. A typology B appears if $p(\omega_i) > \sigma_3$ at ω_i (Case I), and a typology A exists if $p(\omega_i) < \sigma_3$ (Case II). Since $|Y/D_1| = |P/1+L| < \sigma_3$ expresses the attenuation in the plant output of disturbances at its input, the σ_3 -tolerance usually takes values of $0 < \sigma_3 < 1$. It may produce type B or type A bounds. Since the smaller σ_3 and bigger $\{p\}$ produce at low frequencies, type B bounds are more usual at these frequencies. Smaller σ_3 imply stronger B or A bounds which involve a larger disturbance attenuation. The bound appearance for the σ_3 variation is the same than the one for the σ_2 specification in Figure 4.

3.4 Control effort restrictions, $|G/1+L| < \sigma_4$

As shown in Table 4, depending on the relation between the specification, $\sigma_4 = \sigma_4(\omega_i)$, and the plant magnitude $\{p(\omega_i)\}$, the equation (14) offers two different typologies: D when $p(\omega_i) < \sigma_4$ (Case I), and A if $p(\omega_i) > \sigma_4$ (Case II). Note that σ_4 can take any value > 0 , generating type D or A bounds. Smaller σ_4 -values imply tougher D or A bounds, i.e. larger restriction on the control effort, usually required with increasing frequencies. The bound variation looks like the σ_1 -specification influence shown in Figure 3.

3.5 Signal Tracking, $\sigma_{5inf} |L/1+L| < \sigma_{5sup}$

The particular performances of the signal tracking and the disturbance attenuation require two degrees of freedom (Horowitz, 1963). The goal of the controller in the tracking is to reduce the closed loop T -variation, being $|T| = |PG/(1+PG)|$, due to the uncertainty in P . At the same time, G should achieve the remaining performance and stability specifications. At a second design step, a pre-filter F positions $|T_3| = |F| |T|$ according to the upper σ_{5sup} and lower σ_{5inf} models in (5). In the task of the G -controller design, (5) can be rewritten as:

$$\frac{|T_d(j\omega_i)|}{|T_e(j\omega_i)|} \frac{\sigma_{5sup}(\omega_i)}{\sigma_{5inf}(\omega_i)} = \sigma_5(\omega_i) = \sigma_5 \quad (16)$$

assuming that $|T_d(j\omega_i)| > |T_e(j\omega_i)|$. Since $\sigma_{5sup} > \sigma_{5inf}$, then $\sigma_5(\omega_i) > 1$. A σ_5 -decrement is aimed at obtaining a larger reduction in the T -variation for the same uncertainty in P . Then, the specification is more severe, and its QFT bound behaves correspondingly.

According to the bound formula in (15), the relation between $\sigma_5(\omega_i)$ and the plant maximum magnitude uncertainty, $p_{max}/p_{min}(\omega_i)$, determines two different typologies of bounds (see Table 4). The type B for $p_{max}/p_{min} > \sigma_5$ (Case I), and the type A for $p_{max}/p_{min} < \sigma_5$ (Case II). Let's assume p_{max} and p_{min} , the plants with maximum and minimum modulus in $\{p(\omega_i)\}$.

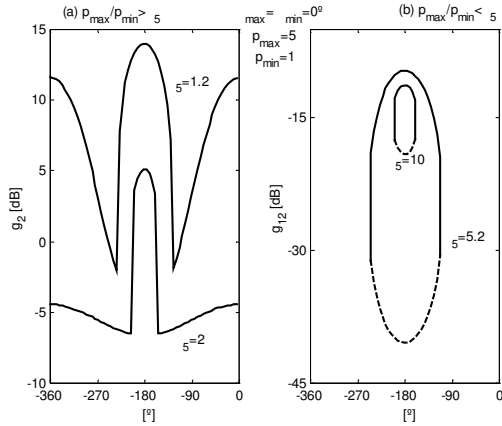


Figure 5: δ influence on its representative bound.

Case I: $p_{\max}/p_{\min} > 5$, G-Bounds of type B. When the specification $\delta = \delta(\omega)$ decreases (major uncertainty reduction required), the magnitude g_2 in (15) decreases at $[-360^\circ, 0^\circ]$, so the bound condition hardens. See Figure 7a.

Case II $p_{\max}/p_{\min} < 5$, G-Bounds of type A. When δ decreases: g_2 increases, g_1 decreases; then, the bound fulfillment toughens. Check Figure 7b. The type A bound relaxation at high frequencies allows closed loop uncertainties larger than those of the open loop, with a negligible feedback effect

4. CONTROLLER DESIGN STRATEGIES

The bounds are the crux of the solution to the robust feedback problem in QFT from two different points of view. Firstly, it is necessary to have bound compatibility. This means that at each frequency ω , there must be a non-null bound intersection amongst the bounds expressing the different k robust specifications. Secondly, it must be possible to loopshape a nominal open loop transmission, $L_o(j\omega) = G(j\omega)P_o(j\omega)$, meeting the non-null bound intersection along the set of frequencies $\{\omega_i\}$.

Gil-Martínez and García-Sanz (2001) partially dealt with the first question. They claimed that to meet multi-objective bounds at a particular frequency simultaneously, type A bounds of any magnitude $g_{1,2}$ can coexist with type B or D bounds. If type B and D bounds coexist, the D-bound g_1 magnitudes should be higher than the B-bound g_2 magnitudes for some ω , relaxing k when necessary. This is a consequence of the trade-offs in the feedback control, which harden in the case of the uncertain systems. The present paper includes some more insights in the matter.

After establishing that the bound typology has a strong influence on the existence of a global solution, note that: (a) the bound typology of the feedback problems $k=1,2$ depends exclusively on the desired behavior k ; (b) in contrast, for $k=3,4$, the bound typology is not only determined by the desired specification, but also by the uncertainty inherent to the system; (c) the feedback benefits at low and medium frequencies

expressed through specifications $k=2,3,5$ usually lead to type B bounds; (d) as a particular case of the feedback problem $k=1$, robust stability constraints appear in any control problem, but fortunately, they provide typology A bounds that are compatible with other typologies.

The bound magnitude g_{12} at each ω and the bound phase range $\Delta\theta_{12}$ are other relevant factors in the bound solution. Section 3 showed the influence of k in this case. As expected, stronger k figures of merit lead to more severe bounds expressing them in QFT (see Figures 3, 4, 5).

Assuming a bound compatibility at each frequency, the bound severity increase due to the harder k tolerances implies a more challenging loopshaping of the controller. The following example proves it. Let's suppose an uncertain plant family $\{P(s) = k/(s+a+1), k \in [1, 5], a \in [1, 5]\}$. Two frequencies are evaluated, a low frequency $\omega_{lf} = 1 \text{ rad/s}$ and a high frequency $\omega_{hf} = 100 \text{ rad/s}$. Figure 6 shows the plant templates, with a nominal plant $P_o(j\omega)$ for $k=1, a=1$. The feedback requirements are: (a) a robust stability with $\gamma_1(\omega) = \gamma_1 = 1.3$ for all frequencies, in particular, $\omega \in \{1, 100\} \text{ rad/s}$. This ensures for the whole set of plants that $PM \geq 45^\circ$ and $GM \geq 5 \text{ dB}$. (b) A robust disturbance rejection at low-medium frequencies, gained with a suitable $\gamma_2(\omega)$ tolerance at $\omega_{lf} = 1 \text{ rad/s}$. This imply a comparison between $\gamma_2^I(\omega_{lf}) = 0.3$ and $\gamma_2^{II}(\omega_{lf}) = 0.1$. The first one assures a disturbance attenuation level of $|Y/D_2| \geq -10.5 \text{ dB}$, and the second one of -20 dB .

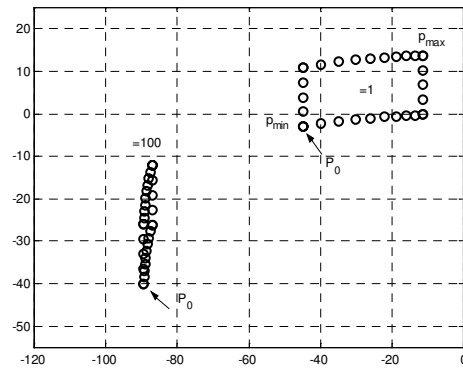


Figure 6: Plant templates.

According to Table 4, since $\gamma_2^{II}(\omega_{lf}) = 0.1$ and $\gamma_2^I(\omega_{lf}) = 0.3$ are lower than 1, they imply typology B bounds. In keeping with Figure 4a and Section 3.2, a decrease in γ_2 implies an increase in the bound height (severity), particularly around 0° and -360° : γ_2^{II} implies a more stringent requirement than γ_2^I in the disturbance attenuation. As a consequence of it, a larger controller static gain is required (see Figure 7). The loopshaping, $L_o = G_1 P_o$, provides a controller for the weaker specification ($\gamma_2^I(\omega_{lf}) = 0.3$):

$$G_1(s) = \frac{4}{s/62 + 1} \quad (17)$$

The strongest performance requirement ($\gamma_{lf}=0.1$) results in $L_{02}=G_2P_0$ or $L_{03}=G_3P_0$ with controllers:

$$G_2(s) = \frac{15}{s/247 + 1} \quad (18)$$

$$G_3(s) = \frac{15(s/96 + 1)}{(s/36 + 1)(s^2/465^2 + 2 \cdot 0.7s/465 + 1)} \quad (19)$$

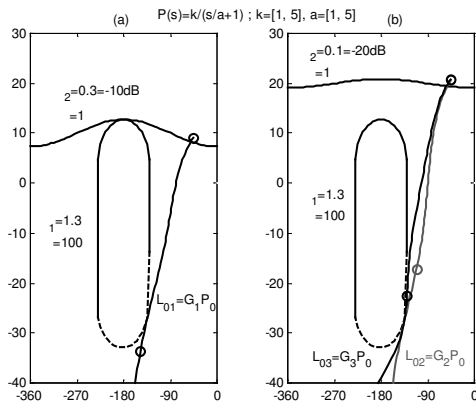


Figure 7: Bounds and loopshaping for robust stability and output disturbance rejection.

An improvement in the performance of the disturbance rejection requires a larger controller static gain (11dB increment between G_2 or G_3 and G_1 gains), claimed by a higher γ_{lf} -bound. The drawbacks turn up at high frequencies (see Figure 7), where $|L_0(\omega_{hf}=100)|$ raises from -33.6 dB for L_{01} to -22.3 dB for L_{03} or to -17 dB for L_{02} . Figure 8 shows some comparative performances between the G_1 and G_2 controllers in the time domain for the nominal plant $P_0=1/s+1$ (plant with the slowest dynamic response). A step disturbance, $D_2(s)=1/s$, appears at $t=1$ sec., being the reference $R(s)=0$. The sensor noise $N(s)$ is simulated by means of a noise disturbance signal with a correlation time 100 times smaller than the fastest dynamics of the system. Figure 8a shows the larger disturbance level attenuation gained with G_2 against G_1 , although it also implies a slightly larger noise amplification at the system output. Figure 8b clearly proves the main feedback drawback: a high frequency $|L_0|$ mainly leads to large $|U/N|$ values that can saturate the actuators (Horowitz, 1973). Better feedback benefits at low frequencies and a relative small high frequency $|L_0|$ (to avoid $|U/N|$ peaks) are simultaneously possible by increasing the complexity of the controller. Compare G_3 with G_2 in Figure 7. However, a higher controller order also implies larger delays in the right control application in practice. The G_2 -controller simplicity implies overdesign in stability margins (23° in PM and 17dB in PM).

5. CONCLUSIONS

The more severe performance and stability specifications in SISO uncertain plants were required, the more stringent feedback trade-offs were proven. Firstly, the bound aggressiveness was studied. Secondly, the controller synthesis difficulties were detailed in a practical example.

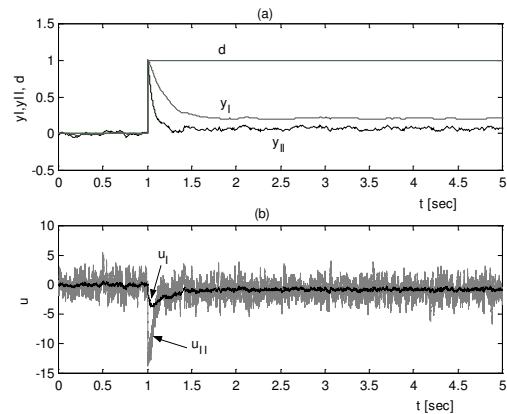


Figure 8: Time domain performance for $P_0(s)=1/s+1$.

ACKNOWLEDGEMENTS

The authors gratefully appreciate the support given by the Spanish 'Comisión Interministerial de Ciencia y Tecnología (CICYT)' under grant DPI2000-0785.

REFERENCES

- Åström, K.J. (2000a). Limitations on control system performance. *Europ. J. Control*, **6**:1, 2–20.
- Åström, K.J. (2000b). Model uncertainty and robust control. *Lect. Notes Iterative Identification & Control Design*, 63–100.
- Bode H.W. (1945). *Network Analysis and Feedback Amplifier Design*, Van Nostrand, New York.
- Borghesani C., Y. Chait and O. Yaniv (1994). *Quantitative Feedback Theory Toolbox User's Guide*. The Math Works Inc., USA.
- Chait Y. and O. Yaniv (1993). Multi-input/single-output computer-aided control design using the Quantitative Feedback Theory. *Int. J. Robust & Non-linear Control*, **3**, 47-54.
- Chen, W. H., and D. J. Ballance, (1999). Plant template generation for uncertain plants in Quantitative Feedback Theory. *ASME J. of Dyn. Sys., Meas., and Control*, **121**, 358-364.
- Gil-Martínez, M., and M. García-Sanz, (2001). Simultaneous meeting of control specifications in QFT. *Proc. 5th International Symposium on QFT and Robust Frequency Domain Methods*, Pamplona, Spain, 193-202.
- Horowitz, I.M. (1963). *Synthesis of Feedback Systems*, Academic Press, New York.
- Horowitz I.M. (1973). Optimum loop transfer function in single-loop minimum-phase feedback systems. *Int. J. Control*, **18**(1), 97-113.
- Horowitz, I.M. (1979). Quantitative synthesis of uncertain multiple input-output feedback systems. *Int. J. Control*, **30**(1), 81-106.
- Houpis, C.H. and S. J. Rasmussen (1999). *Quantitative Feedback Theory. Fundamentals and Applications*. Marcel Dekker, New York.
- Skogestad, S., and I. Postlethwaite (1996). *Multivariable Feedback Control*, Wiley, NY.
- Yaniv O. (1999). *Quantitative Feedback Design of Linear and Non-linear Control Systems*. Kluwer Academic Publishers, Massachusetts, USA.